Supplementary Information for

Modulating thermal conductance across metal/graphene/SiO_2 interface with ion irradiation

Yu Zhao, Yi Tao, Wei Xu, Shuyu Huang, Ming Guo, Jingjie Sha*, Juekuan Yang*, and Yunfei Chen*

Jiangsu Key Laboratory for Design and Manufacture of Micro-Nano Biomedical Instruments, School of Mechanical Engineering, Southeast University, Nanjing 211189, China

Y. Z. and Y. T. contributed equally to this work.

*E-mail: major212@seu.edu.cn; yangjk@seu.edu.cn; yunfeichen@seu.edu.cn.

1. The transferring details of graphene using wet chemical approach

The first step is synthesizing a monolayer graphene on a Cu foil by chemical vapor deposition (CVD) method. Then, the surface of graphene/Cu is coated with polymethyl methacrylate (PMMA) as a support layer [1]. Later, the PMMA/graphene/Cu is immersed into a $FeCl_3$ solution to remove the Cu substrate, and then lifted up from the solution and transferred to the SiO_2/Si substrate. After that, the PMMA is washed away by immersing the whole wafer into an acetone solution. Finally, the graphene/SiO_2/Si is lifted up from the acetone solution and cleaned in the deionized water.

2. The details in the time-domain thermoreflectance measurement

The time-domain thermoreflectance (TDTR) sensitivity to each parameter i is defined as:

$$S_i = \frac{\partial ln(-V_{in}/V_{out})}{\partial ln(i)} \tag{S1}$$

where i is a parameter in the theoretical thermal model, S_i is the sensitivity to a parameter i and $-V_{in}/V_{out}$ is the electric signals collected from the TDTR

measurement. When fitting the measured experimental data with a theoretical thermal model to obtain the thermal conductance across the Al/graphene/SiO_2 interface, there are three unknown fitting parameters, namely the thermal conductivity of Al film k_{Al}, the thermal conductivity of SiO_2 k_{SiO_2} and the thermal conductance across the Al/graphene/SiO_2 interface $G_{Al/graphene/SiO_2}$. The sensitivities of TDTR to three unknown fitting parameters in the measurement are shown in **Fig. S1(a)**. It can be found that the sensitivity of $G_{Al/graphene/SiO_2}$ is high enough for the accurate measurement. **Figure S1(b)** shows the experimental data from the TDTR measurement and the corresponding fitting curves from the theoretical thermal model [2, 3]. It can be clearly seen from **Fig. S1(b)** that the measured experimental data and the theoretical thermal model curves show excellent agreement for the pristine and irradiated graphene.

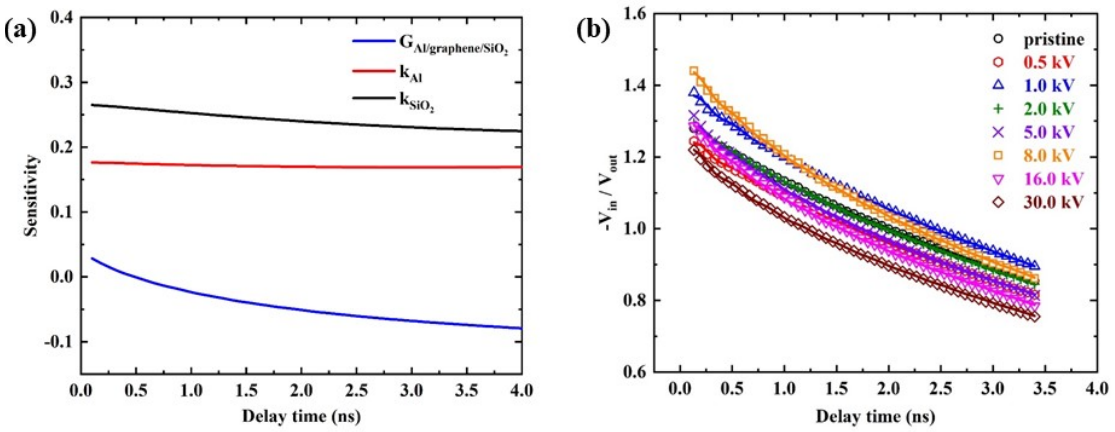

Fig. S1. (a) The TDTR sensitivity curves for the thermal conductance of Al/graphene/SiO_2 interface, the thermal conductivity of Al and the thermal conductivity of SiO_2. (b) The fitting curves for the pristine and irradiated graphene, where the symbols and solid lines denote the measured experimental data and theoretical thermal model fitting curves, respectively.

3. Density functional theory calculations and non-equilibrium Green's function

In order to elucidate the impact of interaction between Al and pristine/irradiated graphene, the density functional theory (DFT) method combined with the non-equilibrium Green's function (NEGF) are utilized to calculate the thermal conductance across the Al/graphene/SiO_2 and Al/irradiated graphene/SiO_2 interfaces, and the corresponding atomic structures are shown in **Fig. S2**. The Vienna *ab initio* simulation package (VASP) is prepared for the DFT calculations [4]. The energy cutoff of 400 eV

is chosen for the plane wave basis sets in the projector augmented wave (PAW) method [5], and the exchange correlation interaction is treated with local density approximation (LDA) [6]. Periodic boundary conditions are followed in the whole interface. To make sure that the unit cells of SiO_2, graphene and Al (111) have the same cross-sectional size, the lattice constants of graphene and Al are set as 2.56 Å and 4.19 Å, which have a lattice mismatch of less than 3%. The optimized equilibrium separations between pristine/irradiated graphene and SiO_2 are set as 1.86 Å, while the equilibrium separations between pristine/irradiated graphene and Al are set as 3.46 Å according to previous report [7]. The second order interatomic force constants (IFCs) of each atomic structure are obtained using the density functional perturbation theory (DFPT) [8] and the phonopy code [9]. Based on the calculated IFCs, the interfacial thermal conductance of Al/graphene/SiO_2 can be calculated according to the NEGF method [7, 10-12].

The Green's function G_D corresponding to the central region can be calculated as [10-12]:

$$G_D = [\omega^2 I - H_D - \Sigma_{LC} - \Sigma_{RC}]^{-1} \tag{S2}$$

where ω is the phonon frequency, H_D is the harmonic matrix of the central region. Σ_{LC} and Σ_{RC} are the self-energy matrices of the left and right contacts. With the Green's function, the transmission function $\Xi(\omega)$ representing the propagation of phonons between two contacts can be calculated as [11, 12]:

$$\Xi(\omega) = \frac{1}{A} Tr(\Gamma_L G_C \Gamma_R G_C^{+}) \tag{S3}$$

where $\Gamma_L = i(\Sigma_L - \Sigma_L^{+})$, $\Gamma_R = i(\Sigma_R - \Sigma_R^{+})$, and "+" denotes the conjugate transpose of the matrix. A represents the cross-sectional area of the heterostructure. The thermal conductance (σ) can be calculated using Landauer formula [10, 11]:

$$\sigma = \int_0^{\infty} \frac{\hbar\omega}{2\pi} N(\omega)\Xi(\omega) d\omega \tag{S4}$$

$$N(\omega) = \frac{\hbar\omega \quad e^{\hbar\omega/k_B T}}{k_B T^2 \quad (e^{\hbar\omega/k_B T} - 1)^2} \tag{S5}$$

where $\hbar$ is the reduced Planck constant, k_B is the Boltzmann's constant, and T is temperature. The thermal conductance obtained from the NEGF method has units of [$Wm^{-2}K^{-1}$].

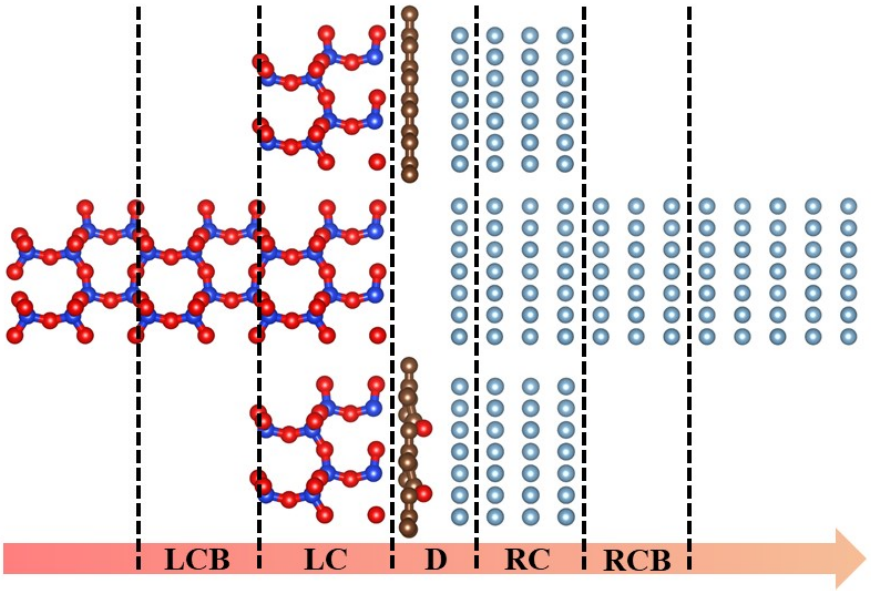

Fig. S2. The schematic diagram of the pristine and irradiated graphene used in the NEGF method. In the schematic diagram, the device (D) region only interacts with the left contact (LC) region and the right contact (RC) region. The left contact bulk (LCB) region only interacts with the LC region, while the right contact bulk (RCB) region only interacts with the RC region. Limited to the computational capability, the IFCs of LC, LCB regions and RC, RCB regions are calculated separately using isolated SiO_2 and Al structures.

The charge density differences shown in **Figs. 6(b)** and **6(c)** of the main text are calculated using the following formula:

$$\Delta\rho = \rho_{Al/graphene/SiO_2} - \rho_{Al} - \rho_{graphene/SiO_2} \tag{S6}$$

where $\rho_{Al/graphene/SiO_2}$, ρ_{Al} and $\rho_{graphene/SiO_2}$ are the charge density for the whole Al/graphene/SiO_2 structure, isolated Al structure and isolated graphene/SiO_2 structure, respectively.

4. The DFT calculations of the irradiated graphene with C-O bonds

According to the X-ray photoelectron spectroscopy (XPS) measurement results in the main text, the concentration percentage of C-O bonds (mostly behave in the form of C-OH) increases from 17.66% to 27.49% after ion irradiation in addition to the formation of C=O bonds. Thus, in order to explore the effect of C-O bonds on the interfacial thermal conductance of Al/graphene/SiO_2, the binding energy between Al and graphene-OH/SiO_2 is calculated using the DFT method. The heterostructures containing the pristine graphene and the irradiated graphene with C-O bonds are shown in **Fig. S3**. The calculation results demonstrate that the binding energy between Al and graphene-OH/SiO_2 is only 0.46 eV nm^{-2}, lower than the value between Al and pristine graphene/SiO_2 (2.34 eV nm^{-2}), which indicates that C-O bonds have a negative effect on the interfacial thermal conductance of Al/graphene/SiO_2. This is because the formed C-O bonds do not destruct the six-membered ring structures of graphene. According to the DFT calculations in the main text and previous literature [7], the enhanced surface adsorption strength induced by electron transfer occurs only when the six-membered ring structures of graphene are destructed.

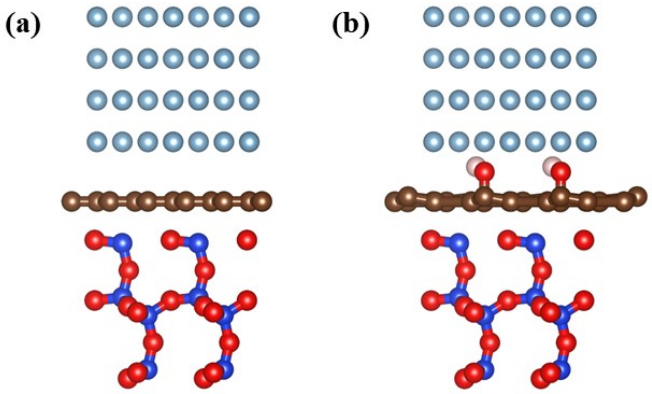

Fig. S3. The structures of DFT calculations for (a) the pristine graphene and (b) the irradiated graphene with C-O bonds. Light blue spheres denote Al atoms, brown spheres denote C atoms, red spheres denote O atoms, blue spheres denote Si atoms and light pink spheres denote H atoms.

References

[1] Y.-C. Lin, C. Jin, J.-C. Lee, S.-F. Jen, K. Suenaga, P.-W. Chiu, *ACS Nano*, 2011, **5**(3), 2362-2368.

[2] D. G. Cahill, *Rev. Sci. Instrum.*, 2004, **75**(12), 5119-5122.

[3] A. J. Schmidt, X. Chen, G. Chen, *Rev. Sci. Instrum.*, 2008, **79**(11), 114902.

[4] G. Kresse, J. Furthmüller, *Comp. Mater. Sci.*, 1996, **6**(1), 15-50.

[5] G. Kresse, D. Joubert, *Phys. Rev. B*, 1999, **59**(3), 1758-1775.

[6] J. P. Perdew, A. Zunger, *Phys. Rev. B*, 1981, **23**(10), 5048-5079.
[7] Y. Tao, C. Wu, H. Qi, C. Liu, X. Wu, M. Hao, Z. Wei, J. Yang, Y. Chen, *Nanoscale*, 2020, **12**(27), 14838-14846.
[8] X. Gonze, C. Lee, *Phys. Rev. B*, 1997, **55**(16), 10355-10368.
[9] A. Togo, F. Oba, I. Tanaka, *Phys. Rev. B*, 2008, **78**(13), 134106.
[10] N. Mingo, L. Yang, *Phys. Rev. B*, 2003, **68**(24), 245406.
[11] J.-S. Wang, J. Wang, J. T. Lu, *Eur. Phys. J. B*, 2008, **62**(4), 381-404.
[12] W. Zhang, T. S. Fisher, N. Mingo, *J. Heat Trans-Trans. ASME*, 2008, **129**(4), 483-491.